

SENSOR MODULE FOR HYDRAULIC BOOM STATE FEEDBACK CONTROL

Janne Honkakorpi¹, Jouni Vihonen² and Juho Mattila¹

¹Tampere University of Technology, Department of Intelligent Hydraulics and Automation, Tampere, Finland

²Tampere University of Technology, Department of Signal Processing, Tampere, Finland

janne.honkakorpi@tut.fi, jouni.mattila@tut.fi, juho.vihonen@tut.fi

Abstract

Hydraulic systems are known to be characterized by poor damping that causes motion oscillations and this limits the obtained hydraulic actuator velocity. Well-known techniques for increasing hydraulic system damping include over-sizing hydraulic actuators, introduction of additional leakages and high-pass filtered pressure or acceleration feedback. The acceleration feedback is a very effective solution but usually the introduction of acceleration sensors increases the overall system cost or the sensors lack adequate robustness against required harsh environmental conditions. In this paper, an implementation of acceleration feedback based on Micro-Electro-Mechanical Systems (MEMS) technology is presented. The proposed solution incorporates a MEMS accelerometer and gyroscope into a sensor module for closed-loop position control and active damping of a hydraulic boom. The performance of the sensor module prototype is experimentally demonstrated on a hydraulic test bench. The results show increased system damping that enables a 47% faster response in the closed-loop position control experiments presented. The achieved steady-state positioning repeatability was within ± 0.06 deg. These results show the feasibility of the proposed solution in such industrial applications, where the productivity of the work is hampered by motion oscillation of the hydraulic actuators.

Keywords: MEMS, signal processing, hydraulic boom, state control

1 Introduction

Active damping of the machine structure has been seen as an important field of study, as it relates directly to operator comfort and productivity of the work. The general trend is to avoid installation of new and separate actuators for oscillation damping as it increases costs and becomes particularly extensive for off-road vehicles due to the required additional installation and control effort. It is therefore preferable to use the existing actuators in an active role to achieve an increase in damping (Rahmfeld and Ivantysynova, 2004).

Feedback from load pressure can be used for keeping the cylinder position close to the given position reference in the presence of disturbances. The use of pressure feedback increases the hydraulic system damping and thus improves the control system performance (Jelali and Kroll, 2003). Acceleration feedback is a control strategy related to pressure feedback. In the case of horizontal planar motion for example, improvement in tracking performance has been achieved by combining acceleration feedback with a nonlinear friction observer (Tafazoli et al. 1996, 1998).

Closed-loop state feedback control is a well-established technique for active vibration damping. The controller is based on position control which is augmented with additional state information about the actuator velocity and acceleration. Assuming a third-order linear time invariant system with ideal feedbacks of position, velocity and acceleration, this controller structure allows for the placing of the closed-loop transfer function poles by adjusting the state feedback (controller) gains. In practice, however, this requires installation of high-resolution position sensors from which the actuator velocity and acceleration estimates are derived by differentiation. This approach introduces unavoidable phase shift and significant noise amplification into the resulting feedback control signals. Furthermore, as the gains of the velocity and acceleration feedback are increased, the system comes increasingly sensitive to the quality of the feedback signals. If the velocity and acceleration signals are noisy, which is the typical case; it will directly translate into chatter of the valve spool.

Micro-electro-mechanical systems, MEMS in short, are components that combine micromechanical struc-

This manuscript was received on 25 November 2011 and was accepted after revision for publication on 5 May 2012

tures and signal conditioning electronics on a single silicon chip. The size of the mechanisms is measured in the micrometre range, which leads to a very small package size. These facts make MEMS sensors an attractive choice in applications where spaces are cramped or where a high degree of chip level integration is required. This paper proposes a novel design solution that incorporates a MEMS tri-axis accelerometer and a single-axis gyroscope into a sensor module prototype for closed-loop position control and active damping of a hydraulic boom. The objective of the developed sensor module is to reconstruct the full state feedback (position, velocity and acceleration) of a hydraulically driven joint. A sensor module with a MEMS rate gyroscope outputs directly the velocity of a joint of a hydraulic manipulator without the need for differentiation of the signal. Moreover, the sensor module requires no direct mechanical contact to a manipulator joint axle, which makes the installation relatively effortless if compared with resolver- or encoder-type installations.

The accelerometer readings provide the instantaneous linear acceleration of motions including the effect of gravitational acceleration field. Thus, resolving the vectorial measurement into a unique instantaneous algebraic estimate of inclination angle becomes limited, if the accelerometer is subjected to high acceleration manoeuvres. The rate-gyroscope is very robust against linear accelerations, but its reading is perturbed by a low-frequency bias term. Different methods have been proposed for measuring (or sensing) inclination angles with MEMS sensors. One approach is to use more than one accelerometer to measure the same hydraulic manipulator joint and subtract the effects of disturbing accelerations from the measurement; see e.g. (Ghassemi et al. 2002; Cheng et al. 2007). Kalman filtering has also been applied when combining accelerometers and gyroscopes; see e.g. (Corpuz et al. 2009; Quigley et al. 2010). However, the assumption that the measurements are corrupted by stationary white noise produces a stationary Kalman filter that is identical, in form to, a so-called complementary filter (Higgins, 1975), which does not require time-domain statistical description for the noise corrupting its input signals. Because of simple representation and analysis in the frequency domain, we consider the complementary filtering (Euston et al. 2008; Honkakorpi, 2010; Mahony et al. 2008) more suitable for MEMS-based inclination angle estimation in this typical fluid power application.

The paper is organised as follows. In Section 2, the state feedback controller tuning theory for position control and active damping of a hydraulic system is presented. Section 3 starts with a detailed presentation of the developed rugged contact-free MEMS sensor module. Then the complementary filtering algorithm design for reconstructing a position estimate and the generation of angular acceleration feedback from MEMS sensor signals is presented. Section 4 presents the experimental set-up. The developed sensor module prototype is experimentally applied into position and damping control of hydraulic test bench set-up in Section 5. Finally, Section 6 provides some relevant conclusions.

2 State Feedback Control

It is widely known that the use of full state feedback (position, velocity and acceleration) can improve the dynamics of a hydraulic servo positioning system. This enables the use of higher loop gains for a better positioning accuracy along with an improved dynamic response.

Hydraulic servo-systems have typically highly non-linear characteristics due to, for example, the compressibility and flow properties of the hydraulic fluid and the friction in the cylinder. However, a linearized model of the system is often relevant from the control perspective, since many applications of different control strategies rely on the use of a linear model (see e.g. Watton, 1989). In the analysis to follow, the modelling of gravitational, inertial, centripetal and frictional terms are put aside and are regarded as external disturbances to the control system. Thus, by assuming a linear time invariant system, a hydraulic servo-system can be modelled with a linear second order open-loop transfer function between valve control input and actuator velocity as shown in Eq. 1:

$$H(s) = \frac{K_{qa} \omega_n^2}{s^2 + 2\delta_n \omega_n s + \omega_n^2} \quad (1)$$

where K_{qa} is the gain from valve control input to cylinder piston speed, δ_n is the natural damping ratio and ω_n is the natural frequency. A simplified closed-loop position control system with full state feedback can then be represented as shown in Fig. 1.

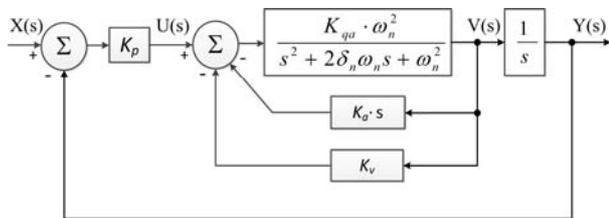


Fig. 1: State-feedback controller

The system consists of an inner second order velocity control loop with feedback gains K_v and K_a , an outer unity feedback, and a gain K_p for the position error. Incorporating the feedback gains K_v and K_a into the transfer function $H(s)$ of Eq. 1 the closed-loop transfer function of the inner velocity control loop becomes

$$\begin{aligned} H_{vel}(s) &= \frac{V(s)}{U(s)} \\ &= \frac{K_{qa} \omega_n^2}{s^2 + (2\delta_n \omega_n + K_a K_{qa} \omega_n^2) s + (1 + K_v K_{qa}) \omega_n^2} \end{aligned} \quad (2)$$

Comparing Eq. 1 and 2 we can see that the servo system with state feedback has a new damping ratio

$$\delta'_n = \frac{2\delta_n + K_a K_{qa} \omega_n}{2\sqrt{1 + K_v K_{qa}}} \quad (3)$$

and a new natural frequency

$$\omega'_n = \omega_n \sqrt{1 + K_v K_{qa}} \quad (4)$$

From Eq. 3 and 4 it can be seen that by increasing the feedback gain K_a the system damping becomes higher. Increasing the value of the feedback gain K_v has the effect of increasing the natural frequency of the system but at the same time, the damping ratio becomes smaller.

The closed-loop transfer function $Y(s)/X(s)$ of the position control loop Fig. 1 can be written as

$$H_{cl}(s) = \frac{Y(s)}{X(s)} \quad (5)$$

with $Y(s) = K_p K_{qa} \omega_n^2$

and $X(s) = s^3 + (2\delta_n \omega_n + K_a K_{qa} \omega_n^2) s^2 +$

$$(\omega_n^2 + K_v K_{qa} \omega_n^2) s + K_p K_{qa} \omega_n^2$$

3 MEMS Sensor Module

The MEMS sensor module developed during the research has tolerance against the harsh working conditions of mobile working machines. This is achieved by casing the embedded module in an epoxy-filled dust- and waterproof aluminium enclosure as shown in Fig. 2. The sensor module dimensions are approximately 110 x 40 x 30 mm. The development work on the sensor has been done entirely at the Department of Intelligent Hydraulics and Automation of Tampere University of Technology. Sensor module MEMS chip is SCC1300-D02 by VTI Technologies. This chip combines a three-axis accelerometer with a one-axis gyro. The top right corner of Fig. 2 illustrates the accelerometer sensing axes X, Y and Z along with the gyro sensing axis Ω in relation to the printed circuit board (PCB). A flux-magnetometer was also considered but not retained due to the vicinity of disturbing metallic structures when the module is mounted on the frame of a mobile machine. The digital output of the accelerometer has a resolution of 0.56 mg per least significant bit (LSB). This translates into a best-case inclination resolution of 0.032 deg when the accelerometer axis is parallel to ground. The digital signal of the gyro has a resolution is 0.02 deg/s per LSB. The MEMS chip has been combined with a 16-bit hybrid signal microcontroller unit (MCU) and line driver chip for implementing low-level data operations and CANopen communication. This makes the sensor module well suited for retrofit-type integration into existing control system platforms of mobile machines.

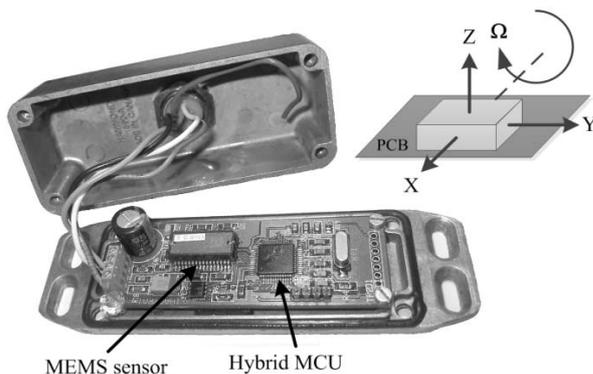


Fig. 2: MEMS sensor module (before filling with epoxy)

3.1 Complementary Filtering of MEMS Data

The key idea of complementary filtering is to combine the advantageous static performance of the accelerometer with the favourable dynamic performance of the gyro.

The accelerometer's noisy inclination reading can be defined as

$$y_a = x + n_a \quad (6)$$

where x is the true inclination angle and n_a the noise of the accelerometer output. The gyroscope's low-noise angular rate signal with bias b is defined as

$$y_g = \dot{x} + n_g + b \quad (7)$$

where the dot operation \dot{x} is the derivative of x producing angular velocity and n_g is the noise of the gyroscope output. The complementary filter for fusing together the accelerometer output of Eq. 6 with the gyroscope output of Eq. 7 is here implemented by a linear feedback system subject to load disturbance. The term n_a contains predominantly high frequency noise just like the term n_g , but its variance is typically much smaller than that of n_a . The bias b is predominantly low frequency disturbance.

Consider the diagram in Fig. 3. The output \hat{x} can be written as

$$\hat{x} = G(s)y_a + [1 - G(s)] \frac{y_g}{s} \quad (8)$$

where

$$G(s) = \frac{C(s)}{s + C(s)} \quad (9)$$

and the complement

$$1 - G(s) = \frac{s}{s + C(s)}. \quad (10)$$

Here $G(s)$ is a low-pass filter associated with the accelerometer's dominantly higher frequency noise and disturbance effects and the complement is associated with the integrated rate measurement Y_g/s to obtain an estimate of the state with dominantly low frequency noise and bias effects. Classical control and filter design techniques can be used for choosing the term $C(s)$. A simple choice is proportional (P) feedback with an integrator (I)

$$C(s) = k_p + \frac{k_i}{s} \quad (11)$$

to make a PI-type system. In this case one obtains a state space filter with the dynamics

$$\dot{\hat{x}} = y_g - \hat{b} + k_p (y_a - \hat{x}), \quad \dot{\hat{b}} = -k_i (y_a - \hat{x}) \quad (12)$$

where k_p determines the crossover frequency chosen as a trade-off based on the low pass characteristics of the accelerometer-based inclination and the low frequency bias characteristics of the gyroscope rate measurements. A non-zero k_i rejects a constant load disturbance b from the output (see e.g. Mahony 2008).

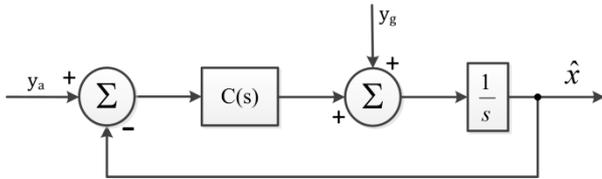


Fig. 3: Complementary filter structure

An illustration of the filter operation is presented in Fig. 4. As can be seen from the figure, due to its high gain, the gyro’s contribution dominates the output of the filter during the starting phase of the movement. Contribution of the accelerometer becomes gradually more significant and reaches the final steady-state value of 3 degrees during which the gyro’s contribution gain has practically decayed to zero. The sum of these signals follows the true position curve during the whole duration of the movement. The reference for true position was here measured from an incremental encoder to be discussed later.

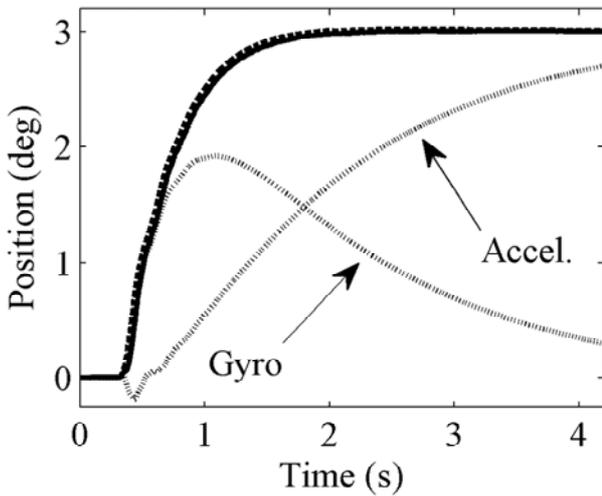


Fig. 4: Complementary filter branch contributions (dotted lines) and the filter output (solid line) versus true position (dashed line)

The average steady-state error of the complementary filter output is typically within ± 0.05 deg. The dynamic error is directly proportional to the speed of the movement, but will remain negligible due to low-bandwidth dynamics of the hydraulic boom, as we shall later discuss.

3.2 Disturbance Attenuation of Angular Acceleration Feedback

The angular acceleration signal is obtained here by simply calculating a discrete difference of the MEMS gyro angular rate

$$d_k = \frac{1}{T_s}(u_k - u_{k-1}) \quad (13)$$

where u_k is the signal input at time k and T_s is the sample time. Note that this introduces the phase-shift as well as the noise amplification as was discussed in Section 1. To improve its quality, two ideas underlie the methodology presented below. The first idea is related to exponential weighting of measurements. The

second is related to robust quantization and further suppression of higher frequency noise, which poses a challenge considering the dynamics of the used hydraulic valve. The servovalve used in the experimental setup has a bandwidth of 60 Hz. Thus, the valve spool will react to any feedback signal noise within this bandwidth.

The differentiation of angular velocity by Eq. 13 is fundamentally of noise amplifying nature. Since delay properties of the acceleration signal are also critical, it is of interest to use higher weights on recent measurements and lower weights on past ones. One way to relate the weights and measurements is through

$$g_k = \sum_{i=0}^{\infty} \gamma_i y_{k-1} \quad (14)$$

where y_k denotes the angular velocity measured at time k . If the weights γ_i are exponential and given by

$$\gamma_i = \alpha(1 - \alpha)^i, \quad 0 < \alpha \leq 1, \quad (15)$$

it is easy to show that the above weighting function can be rewritten in a recursive manner as (Roberts, 1959)

$$g_k = (1 - \alpha)g_{k-1} + \alpha y_k \quad (16)$$

where $g_0 = \mu_0$ is the initial angular velocity typically set to zero. Now the parameter α acts as a forgetting factor and the recursion, called geometric moving average (GMA), has weights decreasing as a geometric progression from the most recent point back to the first. The above makes the GMA an infinite impulse response filter which we tune for noise suppression at the cost of a small delay. Having a delay smaller than the inverse of the natural frequency of the hydraulic system is a necessity, as the control commands of the boom are unknown a priori and the control loop becomes easily unstable. For the parameter α value of 0.75, the recursion impulse response is shown in Fig. 5. It can be deduced that the filter delay is of class one sampling period. Generally, this type of a filter has a memory length of $1/(1 - \alpha)$. For $\alpha = 0.75$, the 4 most recent samples give a significant contribution to the filter output.

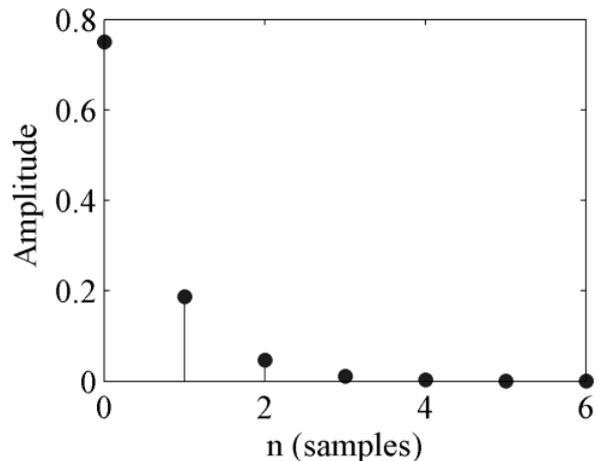


Fig. 5: Impulse response of the GMA filter when α is 0.75

The hydraulic valve dead-zone is a non-linearity that is among the key factors limiting the static and dynamic performance of a closed-loop control system. However, the valve used in the experiments has no

dead-zone but rather a small spool underlap and as such even the smallest non-zero values of the angular acceleration signal may make the boom react. Our straightforward approach to addressing the problem is to create an artificial dead zone by implementing a quantization of close-to-zero values inside the controller. That is, all the GMA filtered angular velocity values in range of ± 0.12 deg/s were set to zero in real-time. The range is application dependent and was chosen empirically by monitoring the GMA filtered signal typical steady-state variation. The result of this operation is shown in graph (b) of Fig. 6.

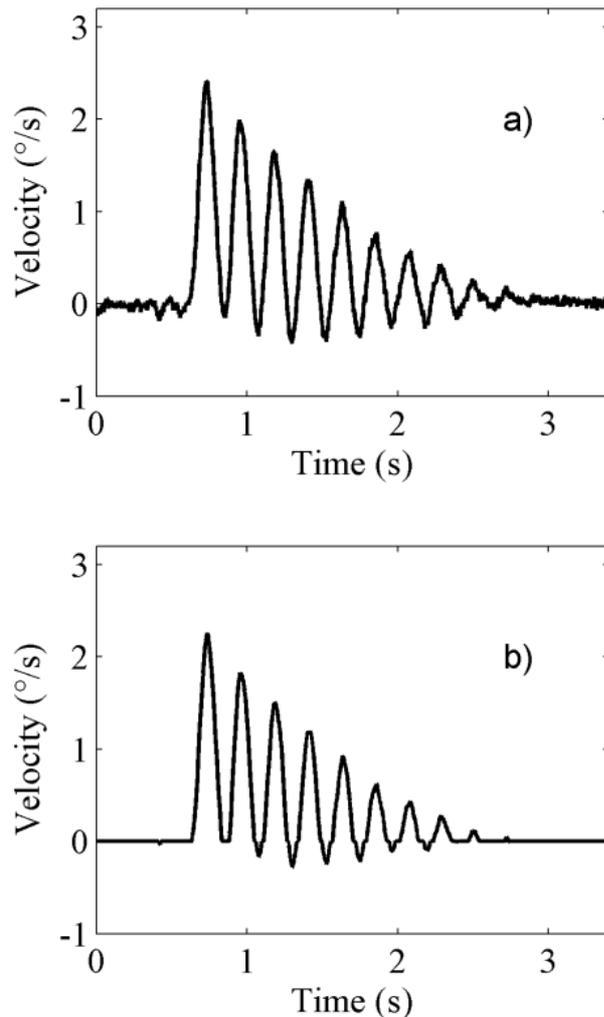


Fig. 6: a) Raw gyro output b) After GMA filter and dead-zone

Since robustness was desired, a median filter of seven consecutive values was used for extra smoothing of the final differentiated angular acceleration, as Fig. 7 shows. The introduced non-linearity effectively cancels small high frequency zero-centred variation in the angular acceleration feedback of the control loop and makes the loop more stable.

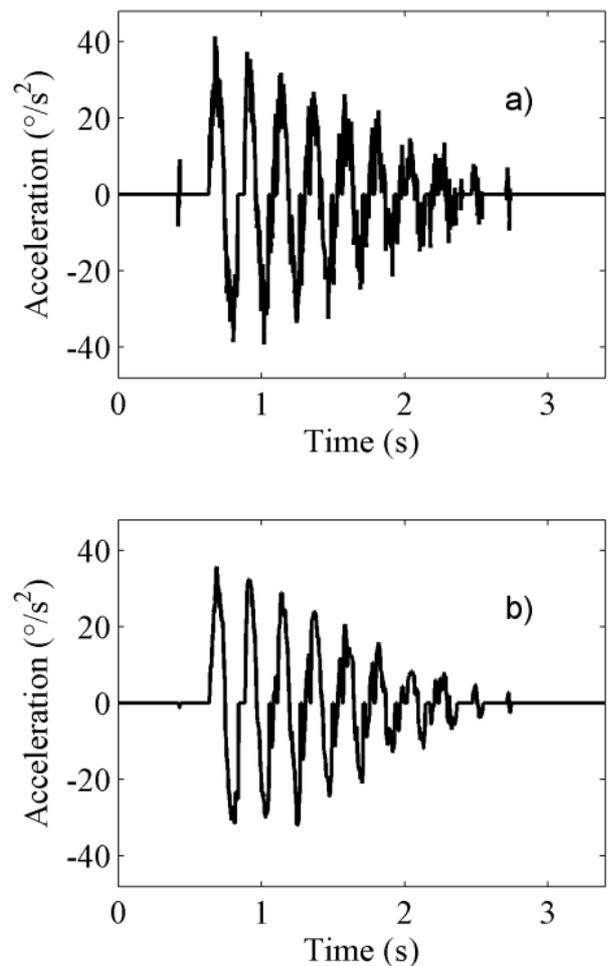


Fig. 7: a) Velocity differentiated into acceleration b) After median filtering

4 Experimental Setup

The experiments for the closed-loop position control were performed on a single-axis hydraulic boom shown in Fig. 8. A test mass of 500 kg was used on the cylinder side of the boom during the experiments. A lift cylinder with a size of 80/45-545 mm was controlled with a hydraulic closed-loop proportional valve that had a nominal flow rate of 24 L/min at a nominal pressure of 3.5 MPa (35 bar) per control notch. With a supply pressure of 21 MPa (210 bar) the cylinder produces a maximum force of 100 kN.

To allow comparison and verification of the developed MEMS sensor performance, a highly accurate Heidenhain incremental encoder with a resolution of 0.00075 degrees per pulse was installed to provide a “true” position reference. The encoder was mounted on the rotating joint pin of the boom assembly. The sensor module was mounted directly on the frame of the boom. A computer-based dSpace DS1103 system was used for the closed-loop control and signal filtering. The sensors were sampled at a rate of 500 Hz ($T_s = 0.002$ s), which was also the controller output update rate. As a remark the authors note, however, that this type of highly accurate encoders are rarely used as feedback sensors on heavy-duty hydraulic manipulators, firstly this is due to the mounting related issues as

discussed in Section 1, and secondly due to the phase-shift and noise amplification issues discussed in Section 3.2.

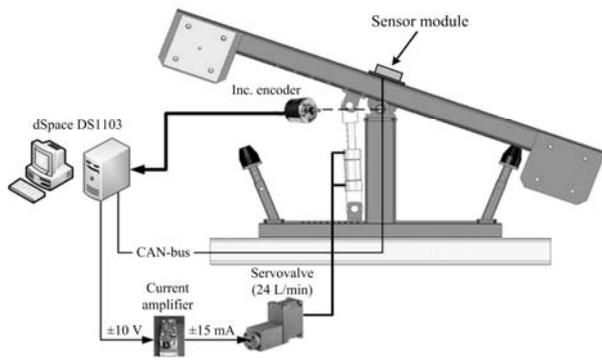


Fig. 8: Test bench setup

The experimental system parameters in Eq. 1 were measured: natural frequency, ω_n , was 28 rad/s; damping ratio was $\delta_n = 0.05$. The measured open-loop velocity gain K_{qa} was 21 deg/s. These measured values yield a theoretical value for marginal stability limit of the proportional feedback gain, K_p , at 0.13 1/s. This so-called critical P-control gain value, K_{cr} , was measured to be 0.1 1/s.

5 Experimental Results of State Feedback Control

The behaviour and performance of the control system was tested initially using stepwise control inputs. A step input is a disturbance to the system that ideally contains all possible excitation frequencies of equal portions in Fourier analysis theory. While such excitation is impossible in any real system, step inputs are useful here for examining the stability and possible oscillatory behaviour of the test bench (Fig. 8). The steady-state accuracy of the closed-loop control system can be also determined along with its rise time (90%). The step sizes we determined to be in the range from 1 degree to 7 degrees.

The controller presented in Fig. 1 was used for proportional and state feedback control. The main aim of the study was to increase the system damping and control the boom oscillations with acceleration feedback (see Eq. 3 and 4). Therefore velocity feedback was omitted ($K_v = 0$) and only partial state feedback was implemented. The acceleration feedback gain K_a was set to zero in the case when pure proportional position control was used. The experiments were first conducted using the encoder as the feedback source and then it was changed to the MEMS sensor. In the case of encoder feedback the angular velocity was first calculated from position with the difference operator of Eq. 13. The same procedure described in Section 3.2 was then used for the generation of angular acceleration from angular velocity for both encoder and MEMS feedback cases.

Initial experiments on the open-loop velocity behaviour of the test bench were performed with a valve command input shown on the top-left corner of Fig. 9.

With no acceleration feedback, the boom velocity exhibits considerable oscillation during the movement as can be expected. The experimental valve command input profile of graph (a) in Fig. 9 represents an approximately typical command input of a mobile machine operator in a working situation. That is to say, it is desired to accelerate the hydraulic actuator quickly to the travelling velocity. The resulting velocity of the boom is shown in graph (b) of Fig. 9.

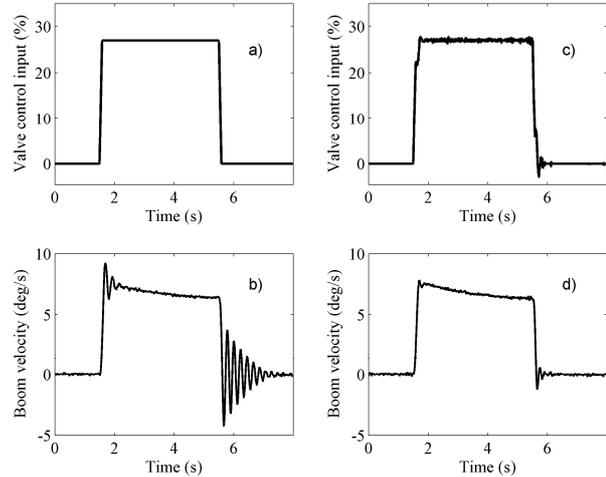


Fig. 9: Valve control input (a) and resulting boom velocity (b) without acceleration feedback and with acceleration feedback (c) and (d)

The velocity response graph (d) of Fig. 9 was achieved by including acceleration feedback to the valve control input as shown in graph(c) of Fig. 9. The response was tuned for maximum damping of velocity oscillations while keeping the acceleration feedback gain within stability limits. In this case, the acceleration feedback gain, K_a , was 0.0008. As it can be seen from Fig. 9, the use of acceleration feedback yields a marked reduction of oscillations especially during the deceleration phase of the movement.

5.1 Proportional Position Control

The following figures present the results of closed-loop position control experiments where the feedback source was changed between the encoder and the MEMS module between experiments. For illustration purposes the measured position values in all the figures are taken from the incremental encoder, as the MEMS position signal follows the encoder position closely throughout the experiments (see Table 1).

Figure 10 shows the results for two different size step inputs when the proportional controller gain K_p was 0.05, which is half of the measured critical gain K_{cr} . As can be seen, the overall dynamic performance with the two different feedback sources is quite similar. The 90 % rise time is approximately 2.1 seconds for the 1 deg and 2.3 seconds for the 5 deg step.

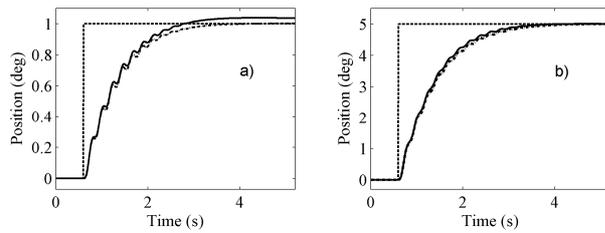


Fig. 10: *P*-control step response a) 1 degree step; $K_p = 0.005$, $K_a = 0$ and b) 5 degree step; $K_p = 0.005$, $K_a = 0$. Encoder feedback (dash-dot), MEMS feedback (solid line)

5.2 State Feedback Position Control

In state feedback control the angular acceleration feedback gain K_a increases the damping of the closed-loop system and enables using a higher value of K_p for more accurate and faster response time without overshooting as can be seen from Fig. 11. For the state feedback experiments the gain K_p was raised to the value of K_{cr} . A suitable value for K_a was found to be 0.00045. Values higher than this started causing instability in the control-loop as the boom behaviour became too sensitive to random variations in the filtered angular acceleration signal. The 90 % rise times are approximately 1.5 seconds for the 1° step and 1.6 seconds for the 5° case. This is an average decrease of some 32 % in the rise time, if compared with the case in Fig 10.

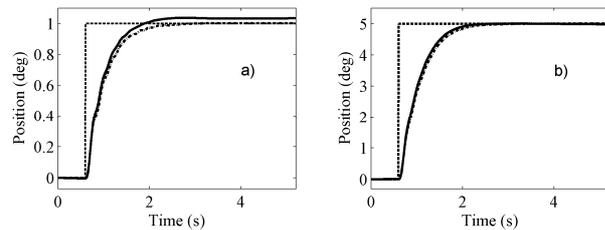


Fig. 11: State control step response a) 1 degree step; $K_p = 0.10$, $K_a = 0.00045$ and b) 5 degree step; $K_p = 0.10$, $K_a = 0.00045$. Encoder feedback (dash-dot), MEMS feedback (solid line)

The steady-state position control errors of all test cases are summarized in Table 1. The error values for each step size are average values of five measurements from which a further overall mean value is calculated. The steady-state error is defined as the difference between the position set point value and true position from encoder. As it is seen, for both feedback cases the state feedback control produces a smaller error. Recalling that the encoder has a resolution of 0.00075 degrees and it operates as a reference, the maximum errors in the table with the encoder feedback source may be considered as an approximation of the error induced by the control loop in question. These errors are ± 0.006 deg and ± 0.004 deg in the proportional (*P*-control) and state-control cases, respectively. Hence, one can deduce that the measured MEMS steady-state positioning error, of class ± 0.06 deg in the both control cases, is almost solely due to the complementary filtering average steady-state error of class ± 0.05 deg (see Section 3.1) which is affected by, for example, linearity and sensitivity errors of the accelerometer. Loosely speak-

ing, as the errors get easily tenfold, this means that the accuracy is limited to the MEMS sensor module linearity and noise specifications. A further improvement can be attained for example by careful recalibration of the MEMS or by developing more sophisticated error-reducing filtering strategies that balance between the various error sources in real-time.

Table 1: Steady-state positioning repeatability (\pm deg) for the indicated position step sizes and the overall mean error per control case

Table 1	1°	3°	5°	7°	mean
P-control, MEMS	0,035	0,15	0,02	0,06	0,066
P-control, encoder	0,002	0,005	0,005	0,006	0,005
State control, MEMS	0,05	0,01	0,03	0,06	0,038
State control, encoder	0,002	0,002	0,003	0,004	0,003

Conclusions

A sensor module combining a MEMS accelerometer and gyroscope data and its application to proportional and acceleration feedback position control of a hydraulic boom was presented. Complementary filtering fused the accelerometer and gyroscope data in such a way that it was usable for position feedback in a closed-loop control system. Angular acceleration feedback was generated from the MEMS gyroscope output by applying differentiation and a so-called GMA-filter. Using this angular acceleration information partial state feedback of the boom was implemented which yielded increased damping in positioning performance; the rise time decreased 32 %, and the steady-state positioning error was on average 42 % smaller. The state feedback control positioning repeatability was on average about ± 0.04 deg with a worst case value of ± 0.06 deg, which one should consider from user and application requirements point of view. Nonetheless, the one degree of freedom preliminary experiments showed that the developed low-cost MEMS-based sensor module is a promising alternative for incremental encoders and resolvers if a robust and easy-to-install sensor for closed-loop position feedback is needed.

Future work will concentrate on applying the MEMS module for closed-loop control in a system with multiple degrees of freedom. A probable candidate is a log forwarder or an excavator boom.

Acknowledgements

This research was funded partly by the Academy of Finland under the project 133273: "Sensor network based intelligent condition monitoring of mobile machinery". Funding was received also from the Graduate School of Concurrent Engineering (GSCE) Tampere. The authors gratefully acknowledge the Academy of Finland and the GSCE Tampere for the financial support. The authors also thank the anonymous reviewers of the International Journal of Fluid Power for their valuable comments.

Nomenclature

a	GMA filter forgetting factor	[-]
b	Gyroscope rate signal bias	[deg/s]
\hat{b}	Complementary filter integrator state	[-]
d_k	Difference operation output	[-]
δ_n	Natural damping ratio	[-]
$(\delta'_n$	Modified natural damping ratio with state feedback	[-]
γ_i	GMA filter weight	[-]
g_k	GMA filter output	[deg/s]
n_a	Accelerometer data noise component	[deg]
n_g	Gyroscope rate data noise component	[deg/s]
K_a	State feedback controller acceleration gain	[s]
K_{cr}	Critical feedback gain	[1/s]
k_I	Complementary filter integrator gain	[1/s ²]
k_p	Complementary filter proportional gain	[1/s]
K_p	State feedback controller proportional gain	[1/s]
K_v	State feedback controller velocity gain	[-]
K_{qa}	Gain from control signal to cylinder speed	[deg/s]
ω_n	Natural frequency	[rad/s]
$(\omega'_n$	Modified natural frequency with state feedback	[rad/s]
Ω	Gyro sensitive axis	[-]
T_s	Sample time	[s]
y_a	Accelerometer inclination angle	[deg]
y_g	Gyroscope output	[deg/s]
x	True inclination (noiseless)	[deg]
\hat{x}	Complementary filter output	[deg]
X	1 st accelerometer sensing axis	[-]
Y	2 nd accelerometer sensing axis	[-]
Z	3 rd accelerometer sensing axis	[-]

References

Cheng, P., Linnarsson, F. and Oelmann, B. 2007. Joint Angular Sensor Based on Distributed Biaxial MEMS Accelerometers. *Proc. 33rd Annual Conference of the IEEE Industrial Electronics Society (IECON)*. Taipei, November 5 - 8, pp. 2242 - 2247.

Corpuz, F. J. O., Lafoteza, B. C. Y., Broas, R. A. L., and Ramos, M. 2009. Design and Implementation of a Closed-Loop Static Balance System for the YICAL Leg 2 Biped. *TENCON 2009 IEEE Region 10 Conference*. January 23 - 26, Singapore.

Euston, M., Coote, P., Mahony, R., Kim, J. and Hamel, T. 2008. A Complementary Filter for Attitude Estimation of a Fixed-Wing UA. *Proc. IEEE/RSJ International Conference on Intelligent Robots and Systems*. Nice, France, pp. 340 - 345.

Ghassemi, F., Tafazoli, S., Lawrence, P. D. and Hashtrudi-Zaad, K. 2002. An Accelerometer-Based Joint Angle Sensor for Heavy-Duty Manipulators, *Proc. IEEE International Conference on Ro-*

botics and Automation. Washington DC, May, pp. 1771 - 1776.

Higgins, W. T. 1975. A Comparison of Complementary and Kalman Filtering. *IEEE Transactions on Aerospace and Electronic Systems*, Vol.11, No. 3, pp. 321 - 325.

Honkakorpi, J. 2010. Application of MEMS Sensor Fusion in Hydraulic Boom Control. *Proceedings of the Post-Graduate Workshop on Intelligent Machines and Transport Systems*. CERN, Switzerland, May 3-7, pp. 27 - 37.

Jelali, M. and Kroll, A. 2003. *Hydraulic Servo-systems: modelling, identification and control. - (advances in industrial control)*. Springer-Verlag London.

Mahony, R., Hamel, T. and Pflimlin, J. - M. 2008. Nonlinear Complementary Filters on the Special Orthogonal Group. *IEEE Trans. on Automatic Control*, Vol. 53, No. 5, pp. 1203 - 1218.

Quigley, M., Brewer, R., Soundararaj, S. P., Pradeep, V., Le, Q. and Ng, A. Y. 2010. Low-cost Accelerometers for Robotic Manipulator Perception. *IEEE/RSJ International Conference on Intelligent Robots and Systems*. Taipei, Taiwan, October 18 - 22.

Tafazoli, S., de Silva, C.W. and Lawrence, P. D. 1996. Friction modeling and compensation in tracking control of an electrohydraulic manipulator. *Proc. IEEE Mediterranean Symposium on New Directions in Control & Automation*. Chania, Greece, June, pp. 375 - 380.

Tafazoli, S., de Silva, C.W. and Lawrence, P.D. 1998. Tracking Control of an Electrohydraulic Manipulator in the Presence of Friction. *IEEE Trans. on Control Systems Tech*, Vol. 6, No. 3, pp. 401 - 411.

Rahmfeld, R. and Ivantysynova, M. 2004. An Overview About Active Oscillation Damping of Mobile Machine Structure. *Int. Journal of Fluid Power*, Vol. 5, No. 2, pp. 5 - 25.

Roberts, S. W. 1959. Control charts based on geometric moving averages. *Technometrics*, Vol. 1, pp. 239 - 250.

Watton, J. 1989. *Fluid Power Systems : modelling, simulation, analog and microcomputer control*. Prentice Hall, New York.



Janne Honkakorpi

Is a researcher at the Department of Intelligent Hydraulics and Automation. He obtained his M.Sc. (Eng.) degree in Electronics from Tampere University of Technology (TUT) in 2007. Currently, he is pursuing his doctoral degree with the support of the Graduate School of Concurrent Engineering (GSCE) Tampere. His research interests include mobile machine control systems, fluid power and sensor networks.



Juho Vihonen

Received his M.Sc. (Eng.) in 2003 and Ph.D. (Tech.) in 2009 both from TUT. He is currently working as a post doc researcher at the Department of Signal Processing. His research interests include recognition-oriented signal processing, nonlinear filtering and their applications to attitude estimation.



Jouni Mattila

Professor, Dr. Tech. Jouni Mattila received M.Sc. (Eng.) in 1995 and Dr. Tech in 2000 both from TUT. He is a professor in Machine Automation at the Department of Intelligent Hydraulics and Automation. His research interests include machine automation and preventive maintenance, and fault-tolerant control system development for advanced machines utilizing lean systems engineering framework.